Award 01-HQ-AG-0019

LIQUEFACTION SUSCEPTIBILITY MAPPING IN MEMPHIS/SHELBY COUNTY, TN

Glenn J. Rix
School of Civil and Environmental Engineering
Georgia Institute of Technology
Atlanta, GA 30332-0355
404-894-2292 (phone), 404-894-2281 (fax)
glenn.rix@ce.gatech.edu

Salome Romero-Hudock
School of Civil and Environmental Engineering
Georgia Institute of Technology
Atlanta, GA 30332-0355
salome.romero@ce.gatech.edu

Research supported by the U.S. Geological Survey (USGS), Department of the Interior, under USGS award number Award No. 01-HQ-AG-0019. The views and conclusions contained in this document are those of the authors and should not be interpreted as necessarily representing the official policies, either expressed or implied, of the U.S. Government.

Non-Technical Summary

Liquefaction is a significant earthquake-related hazard in the Memphis/Shelby County, TN area. In this study, subsurface data from cone penetration tests is used to identify soil deposits that are susceptible to liquefaction. Maps of the Northwest Memphis and Collierville quadrangles have been prepared that show the probability of moderate or major liquefaction-related failures associated with earthquakes of varying magnitudes and levels of peak ground acceleration. Ongoing work is aimed at validating this approach and supplementing it with other types of subsurface data. The results are expected to yield a better understanding of earthquake hazards in the Memphis/Shelby County area.

Award 01-HQ-AG-0019

LIQUEFACTION SUSCEPTIBILITY MAPPING IN MEMPHIS/SHELBY COUNTY, TN

Glenn J. Rix
School of Civil and Environmental Engineering
Georgia Institute of Technology
Atlanta, GA 30332-0355
404-894-2292 (phone), 404-894-2281 (fax)
glenn.rix@ce.gatech.edu

Salome Romero-Hudock
School of Civil and Environmental Engineering
Georgia Institute of Technology
Atlanta, GA 30332-0355
salome.romero@ce.gatech.edu

Abstract

Cone penetration test (CPT) data representing different geologic units in the Memphis/Shelby County, TN area have been collected and used to develop liquefaction potential maps for the Northwest Memphis and Collierville quadrangles. Groundwater levels were obtained from wells in the area. Because a limited number of CPT profiles were available for each geologic region, stochastically simulated profiles were generated to account for the uncertainty within each geologic region based on the statistics of the measured profiles. The resulting probability density functions of cone tip resistance and sleeve friction for each geologic unit were used to calculate the Liquefaction Potential Index (LPI) based on the simplified method. Histograms of LPI were compared with threshold values of LPI to calculate and map probabilities for moderate and major liquefaction-related ground failures for each geologic unit as a function of moment magnitude and peak ground acceleration. Potential errors due to the use of limited data to represent certain geologic units are discussed and an evaluated. Ongoing work to validate this approach and supplement it with more plentiful standard penetration test (SPT) data is briefly described.

Introduction

Urban seismic hazard maps are under development by the U.S. Geological Survey (USGS) for Memphis/Shelby County, Tennessee. Previous efforts to evaluate liquefaction hazards in this area have focused on using qualitative estimates of liquefaction susceptibility based on geologic units (Van Arsdale and Cox, 2003). In this study, we have combined geologic information with quantitative subsurface information compiled by the USGS and limited additional cone penetration test (CPT) data compiled from other researchers to develop a method for estimating the liquefaction potential in a probabilistic framework. The method is based on the liquefaction potential index (LPI). The LPI considers the factor of safety against liquefaction for soil deposits in the upper 20 meters. The factor of safety is weighted as a function of depth to obtain an overall estimate of the liquefaction potential for the entire soil deposit. Liquefaction potential maps are based on the probability of exceeding threshold values of LPI that correspond to moderate and major occurrence of liquefaction. The following sections describe the data and procedures used to prepare trial liquefaction potential maps for the Northwest Memphis and Collierville Quadrangles (Figure 1) in more detail.

CPT Data

Cone penetration test (CPT) data have been used to develop liquefaction resistance criteria (Youd et al., 2001). The main advantage of CPT data is the continuous profile obtained and repeatability of the results (Youd et al., 2001). CPT data were collected for several geologic regions in Shelby County, Tennessee (McGillivray, 2001; Liao et al, 2002). Twenty-nine CPT profiles were obtained from seven sites representing five different geologic regions in Shelby County based on geologic maps developed by the USGS (Figure 2). Table 1 classifies the CPT profiles based on the location within the geologic regions identified by the USGS Memphis Mapping Group. The two measurements of interest for liquefaction analysis are the cone tip resistance (q_t) and the sleeve resistance (f_s). Both measurements were recorded at 0.05-meter increments for all sites except the Trailer Park site, which was recorded at 0.025-meter increments. Liquefaction is assumed to be constrained to the upper 20 meters based on the weighting function used to calculate the liquefaction potential index (Iwasaki et al., 1978; 1982). Therefore, only measurements recorded in the upper 20 meters were considered in the analyses. Figure 3 shows the q_t and f_s profiles for the Shelby County sites.

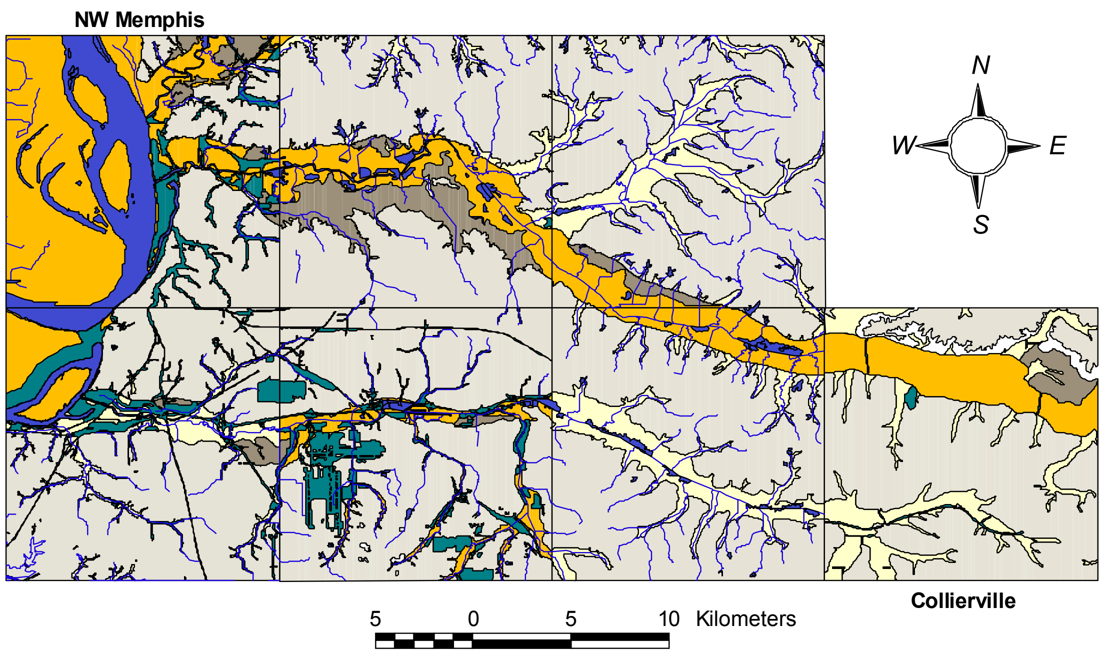

Figure 1 Location of NW Memphis and Collierville quadrangles in Memphis/Shelby County, Tennessee.

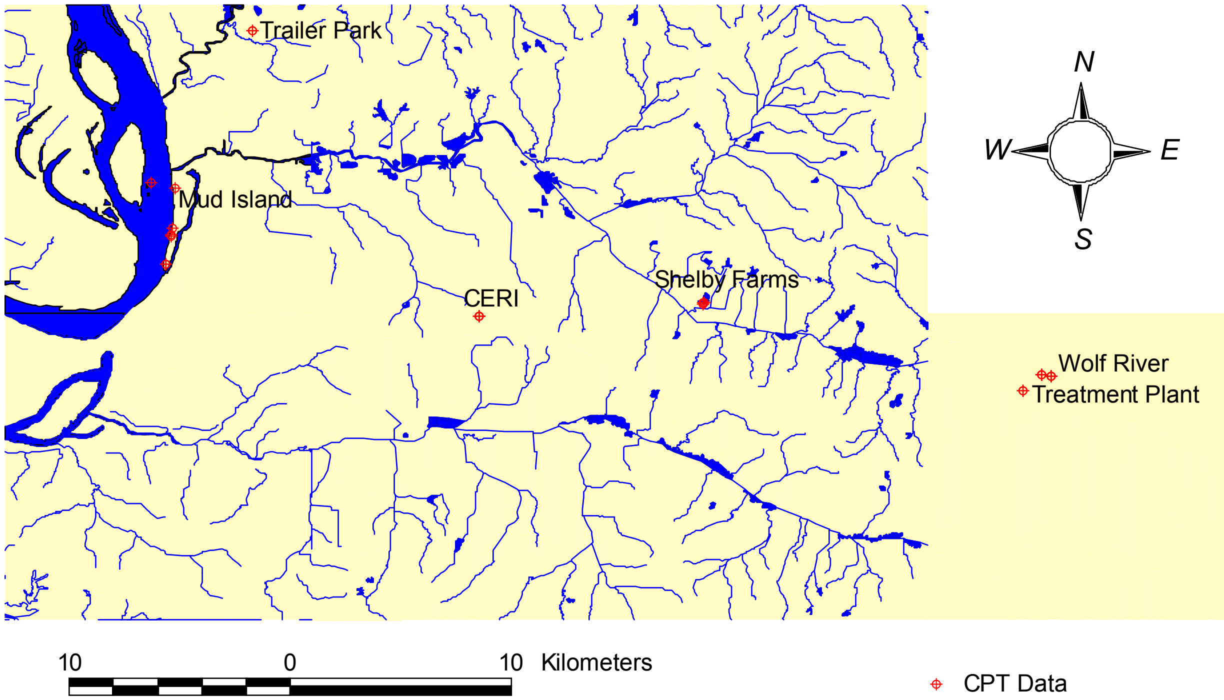

Figure 2 Location of CPT sites in Shelby County, Tennessee.

Table 1 Location of CPT Profiles Based on Geology

Geologic Region	Site	CPT Profile
Af	Mud Island	A11, A12, B, B1, C1, D1, E1
Qa/Qal	Treatment Plant, Wolf River, Shelby Farms	SWG 1, SWG 2 Wolf 1, Wolf 2, Wolf 3, Wolf 4, Wolf 5, Wolf 6, Wolf 7 Shoot A, Shoot B, Shoot C
Ql	CERI, Shelby Forest*	CERI 1, CERI 2, CERI 3, CERI 4 Forst 4, Forst 5, Forst 6, SFOR 1
Qtl	Trailer Park	TRPK 1, TRPK 2

* Site located outside of mapping region but within Shelby County

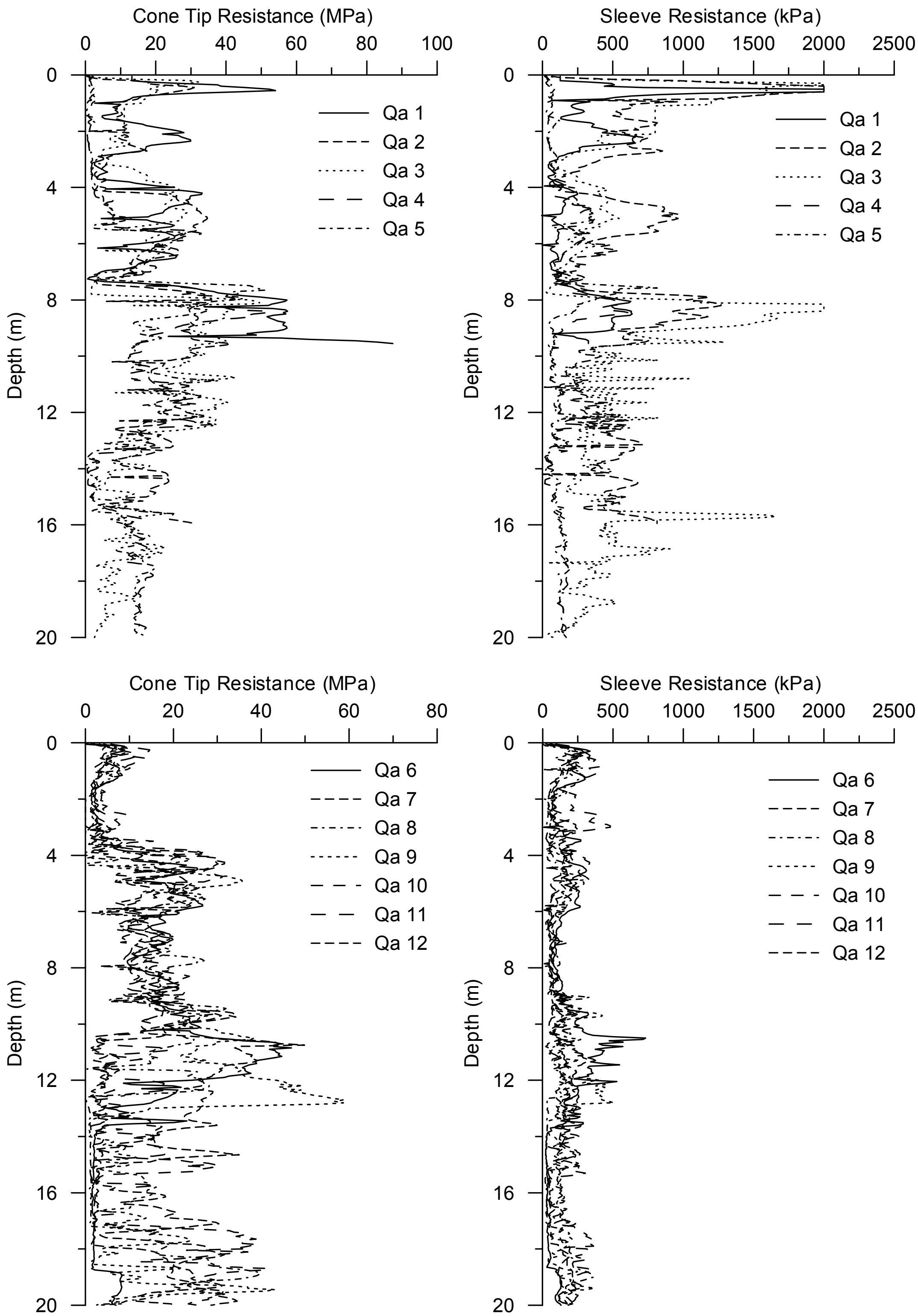

Figure 3 CPT profiles for Shelby County, Tennessee sites

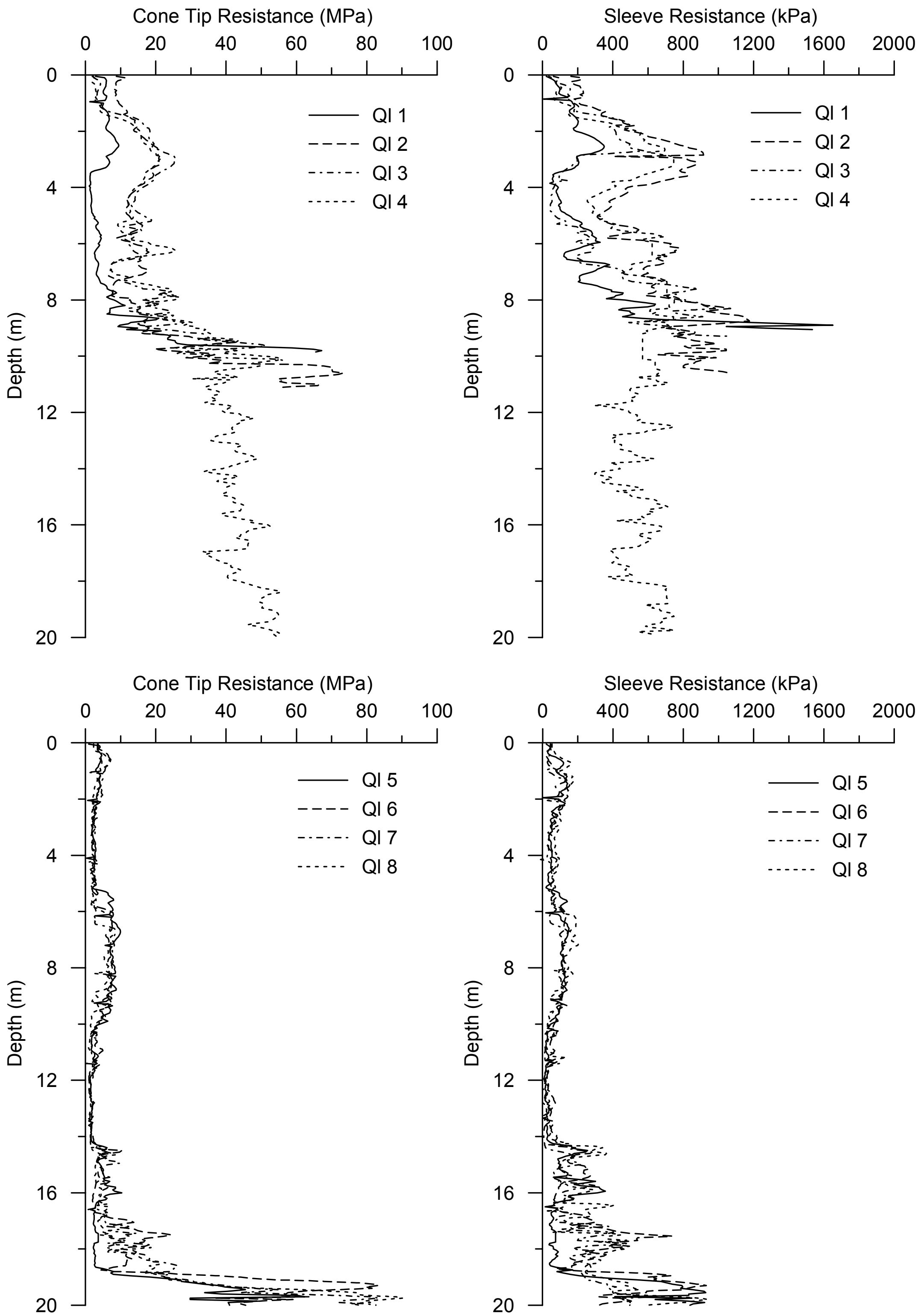

Figure 3 (cont'd) CPT profiles for Shelby County, Tennessee sites

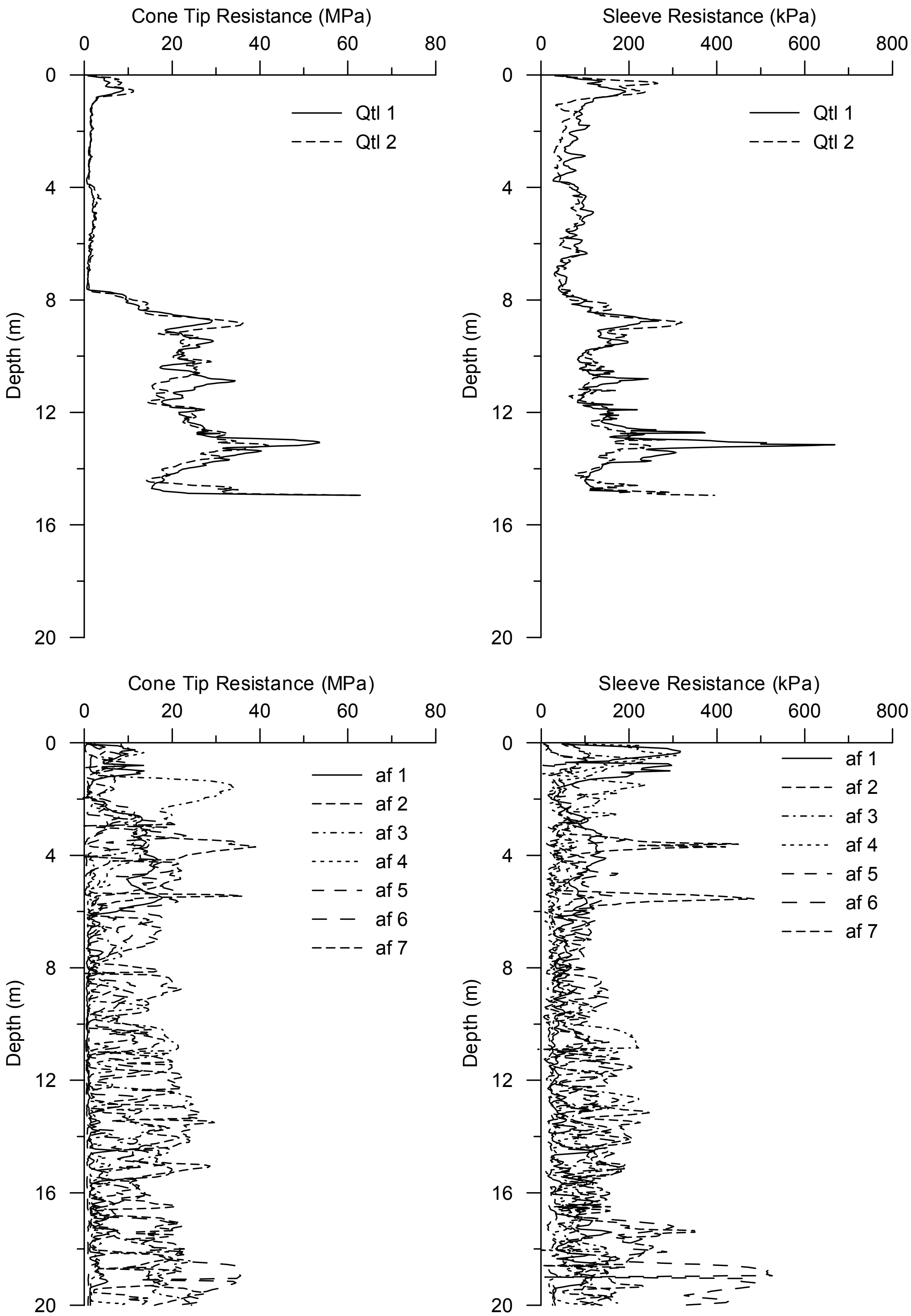

Figure 3 (cont'd) CPT profiles for Shelby County, Tennessee sites

Groundwater Table

Liquefaction susceptibility depends on the location of the groundwater table. Hwang et al. (1999) compiled subsurface information for Shelby County. Based on the subsurface data, 464 groundwater wells were used to produce a contour map of the depth to the groundwater table. Contour maps for the Collierville and NW Memphis Quadrangles are shown in Figure 4.

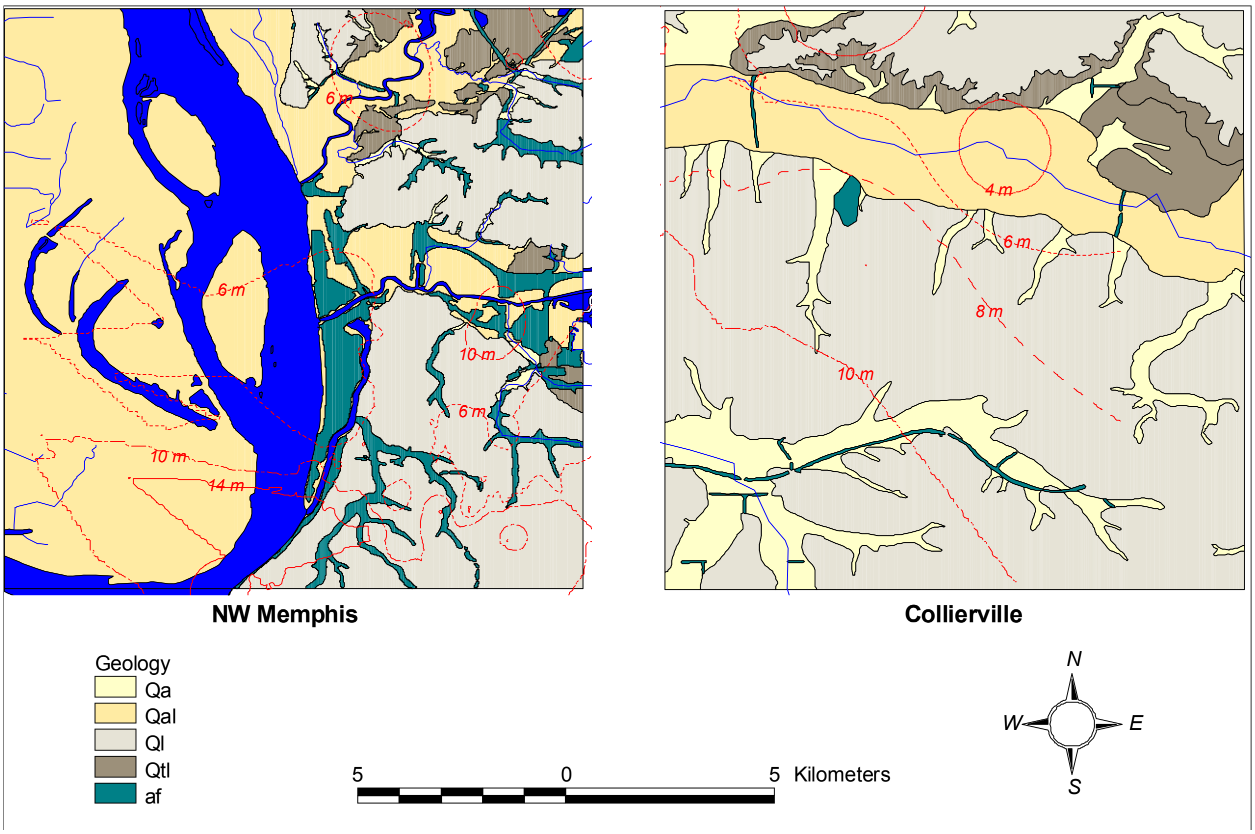

Figure 4 Depth to the groundwater table in the NW Memphis and Collierville quadrangles (based on Hwang et al., 1999).

Simulation of CPT Profiles

Since only a limited number of CPT profiles were available for each geologic region, stochastically simulated profiles were generated to account for the uncertainty within each geologic region based on the statistics of the measured profiles. The autocorrelation between measurements recorded at adjacent depth increments was used to produce more realistic simulated CPT profiles.

Simulated profiles were generated by subdividing each cone penetration tip resistance (q_t) profile into separate layers by visually inspecting the q_t profile to identify depth intervals with similar characteristics. For each layer, the lognormal mean and lognormal standard deviation were determined. The mean and standard deviation were used to calculate a standard normal residual value of q_t using the following expression:

$$q_{norm} = \frac{\log_{10}(q_t) - \mu_{\log_{10}(q_t)}}{\sigma_{\log_{10}(q_t)}}$$

where μ denotes the mean and σ denotes the standard deviation. An example is shown in Figure 5. The standard normal residual values of q_t are approximately normally distributed as shown in Figure 6.

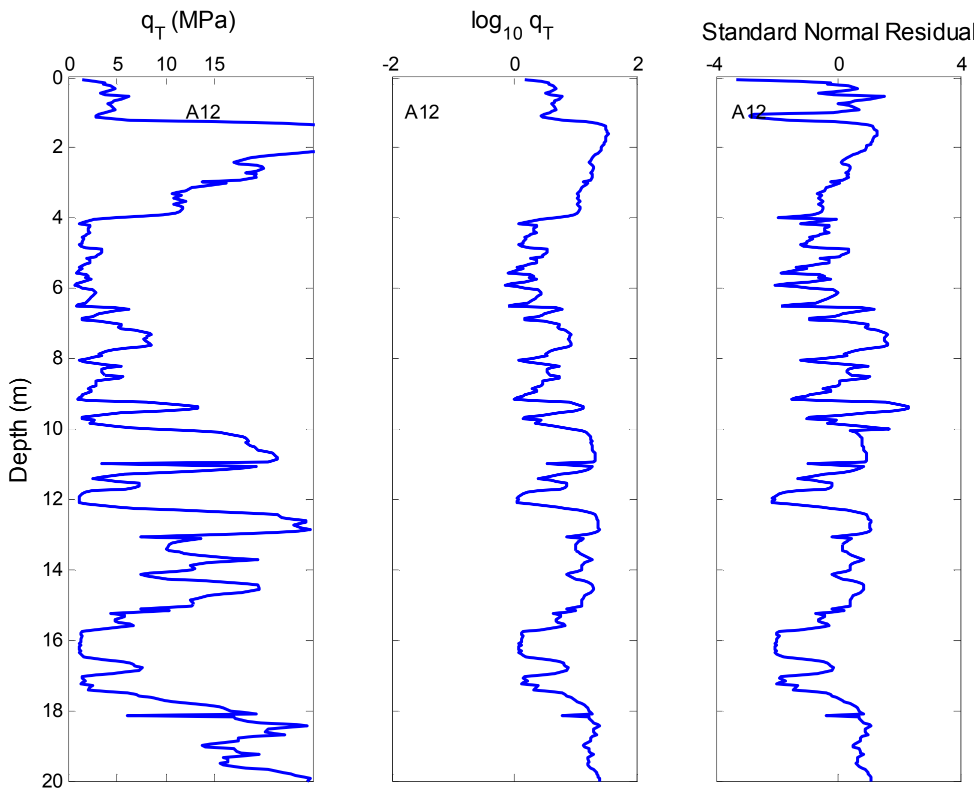

Figure 5 Example of (a) q_t, (b) $\log_{10}(q_t)$, and (c) standard normal residual q_t profiles for Mud Island Site A12.

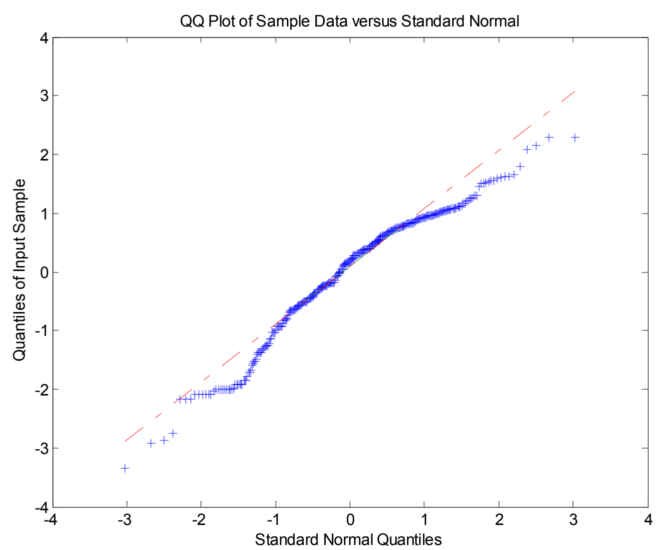

Figure 6 Quantile-quantile plot of standard normal residual q_t data

The autocorrelation function of the standard normal residual q_t profile was calculated to determine the spatial correlation of cone penetration data in the vertical direction. An example is shown in Figure 7. The experimental autocorrelation function was fitted using an exponential model described by:

$$\rho(h) = \exp\left(\frac{-3h}{a}\right)$$

where ρ is the correlation coefficient, h is the spatial lag, and a is the effective range (Deutsch and Journal, 1998). The effective range characterizes the spatial correlation of q_t.

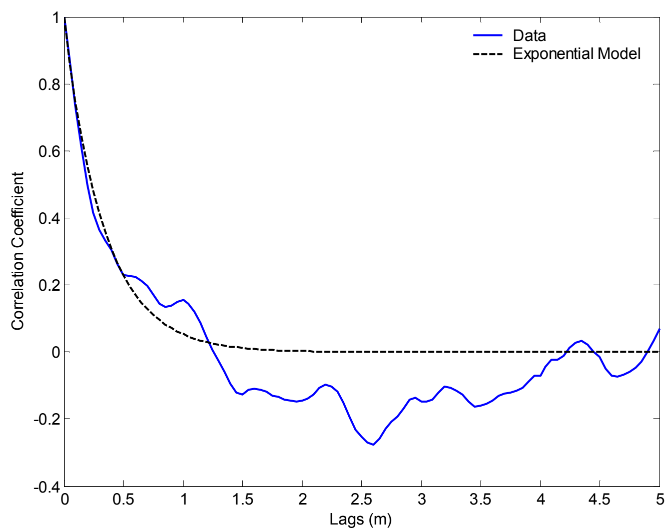

Figure 7 Experimental autocorrelation function and exponential model

Unconditional simulations of each q_t profile (defined by the mean and standard deviation of each layer and the effective range) were generated using the LU decomposition algorithm contained in GSLIB, a geostatistical software library (Deutsch and Journel, 1998). Taken as whole, the simulated profiles have the same statistical properties (mean, standard deviation, and autocorrelation structure) as the corresponding experimental q_t profile. Twelve hundred simulated profiles were generated for each geologic region.

Evaluation of the liquefaction resistance using CPT data also requires profiles of the sleeve friction. As such, it was necessary to jointly simulate f_s profiles. This was achieved by calculating the probability density function (pdf) for f_s conditional on q_t as shown in Figure 8. For each value of q_t, the corresponding value of f_s was randomly selected using the probability density function. Figure 9 shows an example of the simulated profiles generated using the autocorrelation method described.

Simplified Approach

Youd et al. (2001) summarize the current state-of-the-art of methods for evaluating liquefaction resistance based on the simplified method. The seismic demand is given by the cyclic stress ratio (CSR):

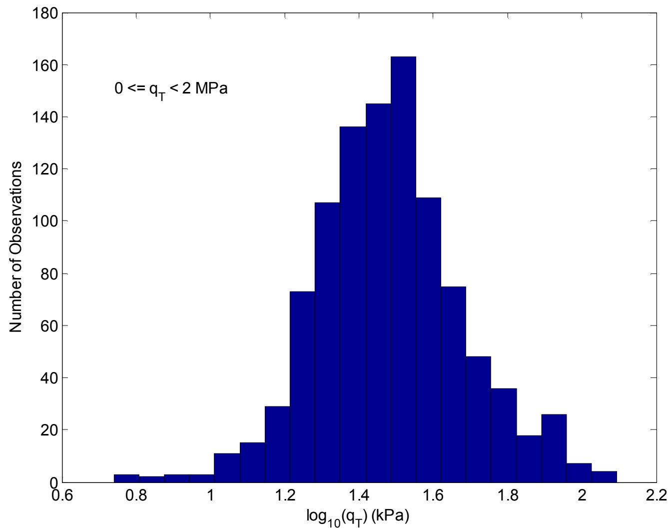

Figure 8 Probability density function for f_s conditional on q_t.

$$CSR = \frac{\tau_{av}}{\sigma'_{vo}} = 0.65\left(\frac{a_{\max}}{g}\right)\left(\frac{\sigma_{vo}}{\sigma'_{vo}}\right)r_d$$

where the stress reduction coefficient, r_d, is a function of depth, z, and is approximated by the following equation:

$$r_d = \frac{1.000 - 0.4113z^{0.5} + 0.04052z + 0.001753z^{1.5}}{1.000 - 0.4177z^{0.5} + 0.05729z - 0.006205z^{1.5} + 0.001210z^{2}}$$

The cyclic resistance ratio (CRR) defines the liquefaction resistance of the soil and is based on the results of cone penetration tests (CPT). The CRR delineates which sites will liquefy and which will not and is given as:

$$(q_{c1N})_{cs} < 50 \qquad CRR_{7.5} = 0.833\left[\frac{(q_{c1N})_{cs}}{1000}\right] + 0.05$$

$$50 \le (q_{c1N})_{cs} < 160 \qquad CRR_{7.5} = 93\left[\frac{(q_{c1N})_{cs}}{1000}\right]^3 + 0.08$$

where $(q_{c1N})_{cs}$ is the cone penetration resistance corrected to a clean sand and normalized to 100 kPa. The normalized cone tip resistance is corrected for overburden stress as:

$$q_{c1N} = C_Q\left(\frac{q_c}{P_a}\right)$$

$$C_Q = \left(\frac{P_a}{\sigma'_{vo}}\right)^n$$

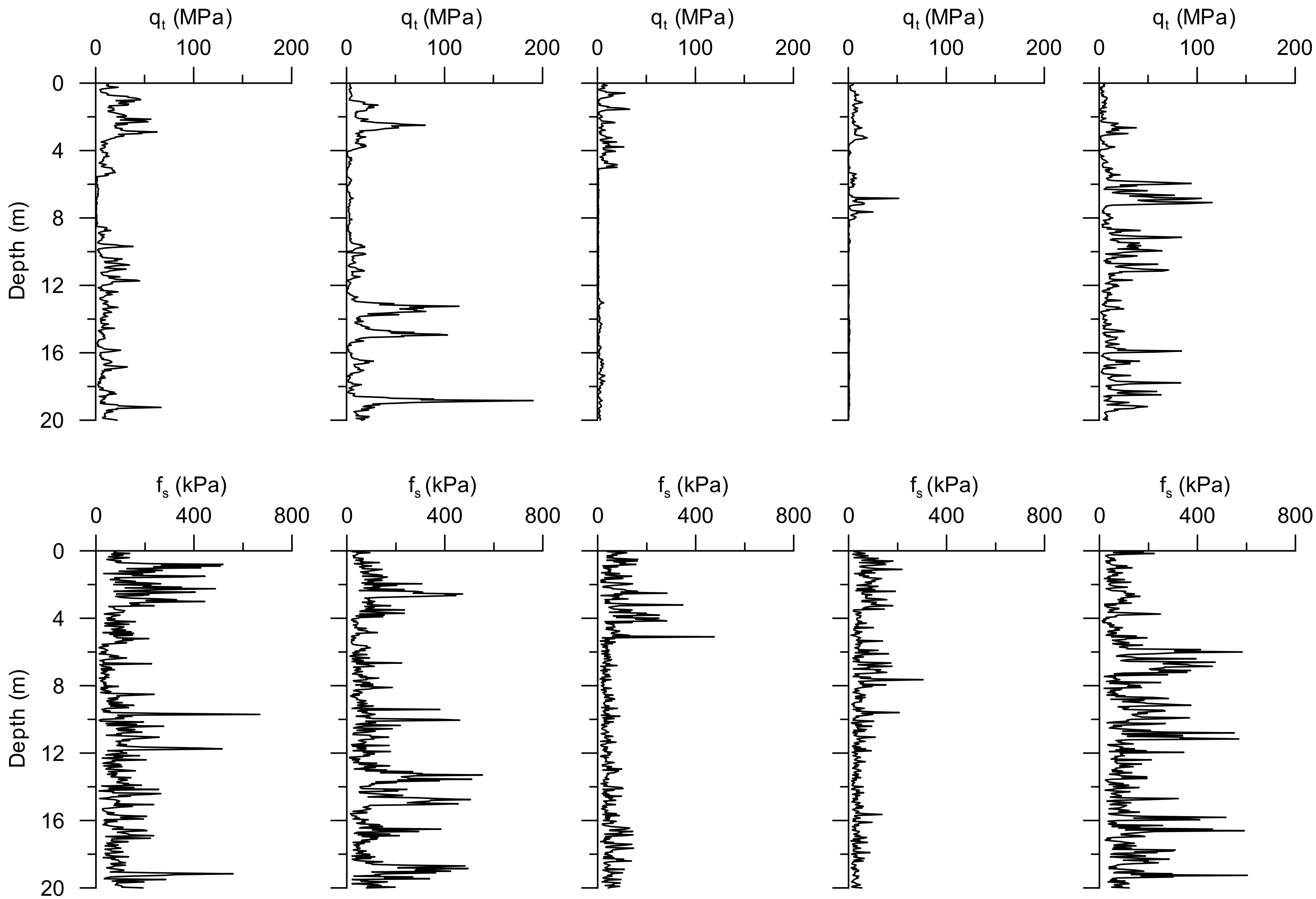

Figure 9 Simulated profiles based on autocorrelation method for generating CPT profiles.

where P_a is 100 kPa and q_c is the cone tip resistance measured in the field. To correct for fines content, a correction factor, K_c, is applied that is a function of the soil behavior type index, I_c. I_c is given as:

$$I_c = \left[(3.47 - \log Q)^2 + (1.22 + \log F)^2\right]^{0.5}$$

$$Q = \left[\frac{q_c - \sigma_{vo}}{P_a}\right]\left[\frac{P_a}{\sigma'_{vo}}\right]^n$$

$$F = \left[\frac{f_s}{q_c - \sigma_{vo}}\right] \times 100\%$$

where f_s is the measured sleeve resistance, and n is a function of the type of soil that is obtained by iterating as discussed in Youd et al. (2001). The normalized cone tip resistance is corrected by:

$$(q_{c1N})_{cs} = K_c q_{c1N}$$
$$K_c = 1.0 \qquad I_c \le 1.64$$
$$K_c = -0.403 I_c^4 + 5.581 I_c^3 - 21.63 I_c^2 + 33.75 I_c - 17.88 \qquad I_c > 1.64$$

Figure 10 shows the typical relationship of CSR and CRR for a site in Shelby County. The factor of safety against liquefaction is calculated as:

$$FS = \left(\frac{CRR_{7.5}}{CSR}\right) \times MSF$$

where $CRR_{7.5}$ is the cyclic resistance ratio for a magnitude 7.5 earthquake and MSF is the magnitude scaling factor that corrects for moment magnitudes other than 7.5. Several MSF have been proposed (Youd et al. 2001). For this study, the MSF proposed by Idriss (1995) were selected. Figure 11 shows the factor of safety against liquefaction for a site in Shelby County as a function of depth.

Liquefaction Potential Index

The liquefaction potential index (LPI) is defined as (Iwasaki et al., 1978; 1982):

$$LPI = \sum_{i=1}^{n} w_i S_i H_i$$

where *w* is the depth dependent weighting function given as:

$$w_i(z) = 10 - 0.5z$$

S is the degree of severity calculated as:

$$S = 1 - FS \qquad 0 \le FS \le 1$$
$$S = 0 \qquad FS > 1$$

where *FS* is the factor of safety defined as the ratio of the cyclic resistance ratio to the cyclic stress ratio, and *H* is the thickness of the layer of interest.

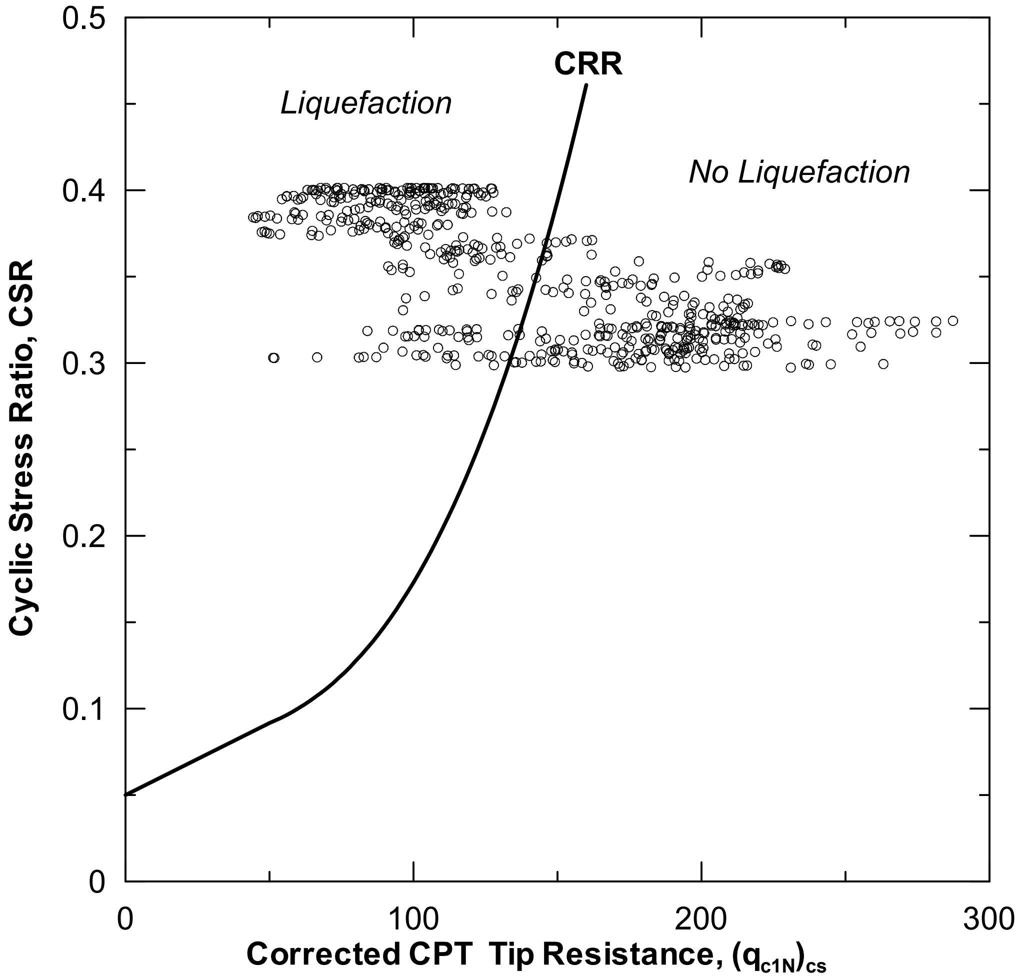

Figure 10 Relationship between cyclic stress ratio (CSR), corrected CPT tip resistance, and cyclic resistance ratio (CRR).

Results

The liquefaction potential index was calculated for each of the 1200 simulated profiles in each geologic region. Results were obtained for moment magnitudes of 6.5 and 7.5 and peak ground acceleration values of 0.2 g, 0.3 g, 0.4 g, and 0.5 g. Similarly, results were obtained for several values of depth to the groundwater table. Figure 12 shows typical histograms of the liquefaction potential index for each geologic region. The percentage of profiles exceeding LPI values of 5 and 15 was calculated since these two values correspond to moderate occurrence and major occurrence of liquefaction, respectively. Based on Iwasaki (1982), the liquefaction severity classifies the LPI to define the potential for liquefaction as shown in Table 2. The probability of exceeding an LPI of 5 and 15 is listed in Table 3 for the Northwest Memphis and Collierville quadrangles for the two moment magnitudes and four peak ground acceleration values. An average depth to the groundwater table was assumed for each quadrangle based on the available data. However, the contour map of depth to the groundwater table may also be used to produce more site-specific liquefaction potential. The results in Table 3 were used to produce liquefaction potential maps.

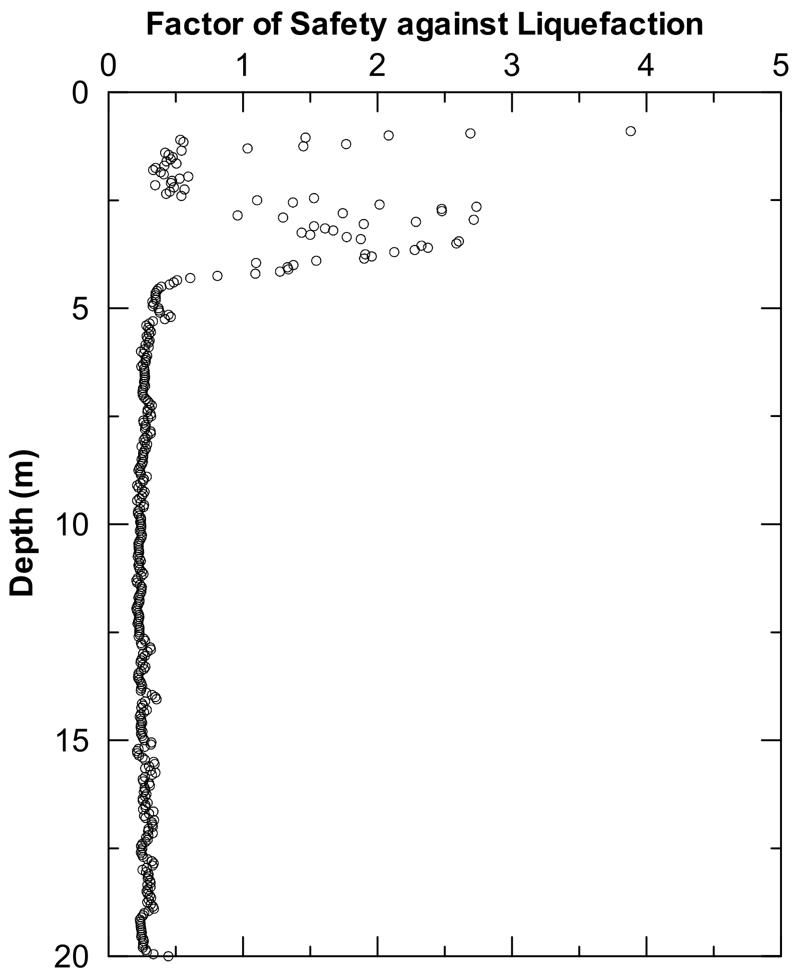

Figure 11 Factor of safety against liquefaction versus depth.

Table 2 Liquefaction Severity as a function of Liquefaction Potential Index

Liquefaction Severity	LPI
Little to none	LPI = 0
Minor	0 < LPI < 5
Moderate	5 < LPI < 15
Major	15 < LPI

Liquefaction Potential Maps

Based on the results of each geologic region, liquefaction potential maps are produced. The results given in Table 3 were joined with the geologic maps for the Northwest Memphis and Collierville quadrangles. The LPI values were joined to the geologic maps by the geology field. Therefore, liquefaction potential maps can be produced for each quadrangle for various combinations of moment magnitude, peak ground acceleration, and LPI value.

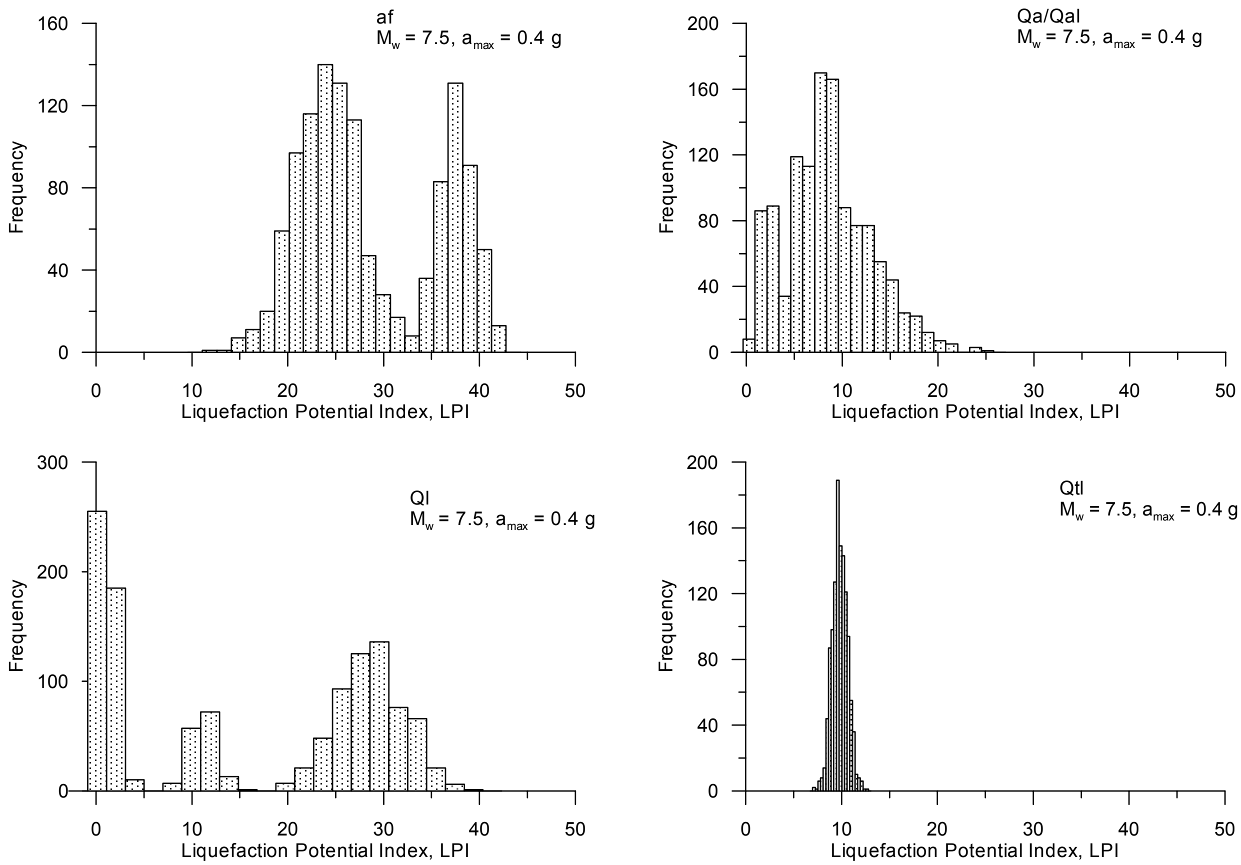

Figure 12 Typical histograms for each geologic region for a given moment magnitude (M_w) and peak ground acceleration (a_{max})

Figures 13 and 14 show the liquefaction potential for the Northwest Memphis quadrangle for a moment magnitude of 7.5 and a peak ground acceleration of 0.4 g. Figure 13 shows the probability of exceeding an LPI of 5 whereas Figure 14 shows the probability of exceeding an LPI of 15. The regions classified as fill have the highest LPI values. Fill is assumed to be placed with minimal ground improvement. In other words, the results for the fill do not consider ground modification techniques that would improve the strength and liquefaction resistance of the material. Figures 15 and 16 show the liquefaction potential for the Collierville quadrangle for a moment magnitude of 7.5 and a peak ground acceleration of 0.4 g. Figure 15 shows the probability of exceeding an LPI of 5 and Figure 16 shows the probability of exceeding an LPI of 15.

Table 3 Probability of Exceeding LPI of 5 and 15 for depth to groundwater table of 6 m

Quadrangle	Geology	Moment Magnitude, M_w	Peak Ground Acceleration, a_{max} (g)	Probability of Exceeding LPI of 5, P [LPI > 5] (%)	Probability of Exceeding LPI of 15, P [LPI > 15] (%)
NW Memphis	af	6.5	0.2	0	0
			0.3	78	0
			0.4	100	53
			0.5	100	95
		7.5	0.2	71	0
			0.3	100	73
			0.4	100	99
			0.5	100	100
	Qa/Qal	6.5	0.2	0.083	0
			0.3	2.2	0
			0.4	16	0.083
			0.5	60	2.2
		7.5	0.2	1.8	0
			0.3	29	0.42
			0.4	80	8.7
			0.5	88	36
	Qtl	6.5	0.2	0	0
			0.3	0	0
			0.4	0	0
			0.5	99	0
		7.5	0.2	0	0
			0.3	0.42	0
			0.4	100	0
			0.5	100	83
	Ql	6.5	0.2	0	0
			0.3	46	0
			0.4	50	25
			0.5	62	50
		7.5	0.2	39	0
			0.3	52	43
			0.4	63	50
			0.5	65	62

Table 3 (continued) Probability of Exceeding LPI of 5 and 15 for depth to groundwater table of 6 m

Quadrangle	Geology	Moment Magnitude, M_w	Peak Ground Acceleration, a_{max} (g)	Probability of Exceeding LPI of 5, P [LPI > 5] (%)	Probability of Exceeding LPI of 15, P [LPI > 15] (%)
Collierville	af	6.5	0.2	0	0
			0.3	78	0
			0.4	100	53
			0.5	100	95
		7.5	0.2	71	0
			0.3	100	73
			0.4	100	99
			0.5	100	100
	Qa/Qal	6.5	0.2	0.083	0
			0.3	2.2	0
			0.4	16	0.083
			0.5	60	2.2
		7.5	0.2	1.8	0
			0.3	29	0.42
			0.4	80	8.7
			0.5	88	36
	Qtl	6.5	0.2	0	0
			0.3	0	0
			0.4	0	0
			0.5	99	0
		7.5	0.2	0	0
			0.3	0.42	0
			0.4	100	0
			0.5	100	83
	Ql	6.5	0.2	0	0
			0.3	46	0
			0.4	50	25
			0.5	62	50
		7.5	0.2	39	0
			0.3	52	43
			0.4	63	50
			0.5	65	62

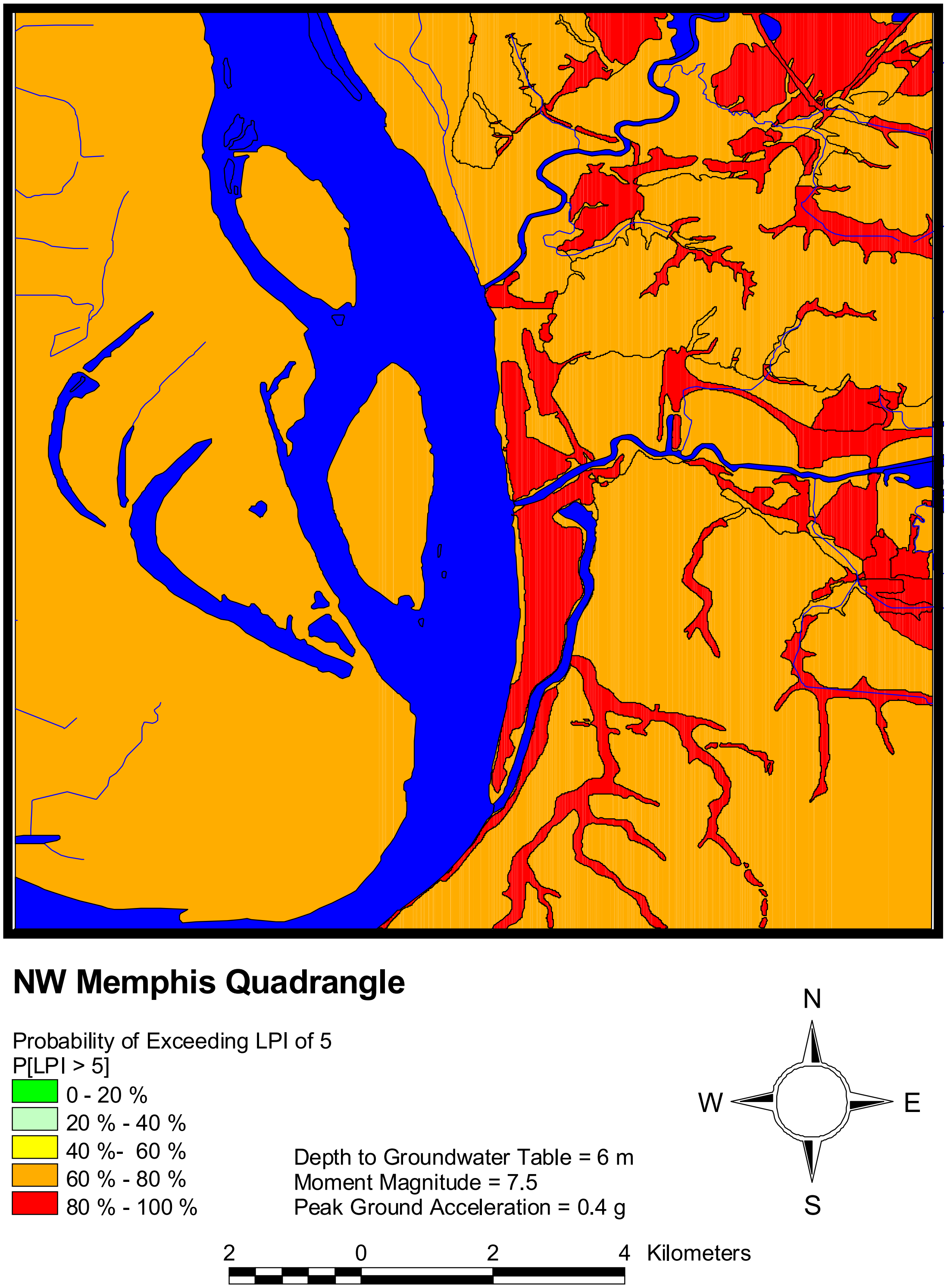

Figure 13 Liquefaction potential map based on liquefaction potential index (LPI) exceeding 5 for NW Memphis quadrangle for a moment magnitude of 7.5 and a peak ground acceleration of 0.4 g.

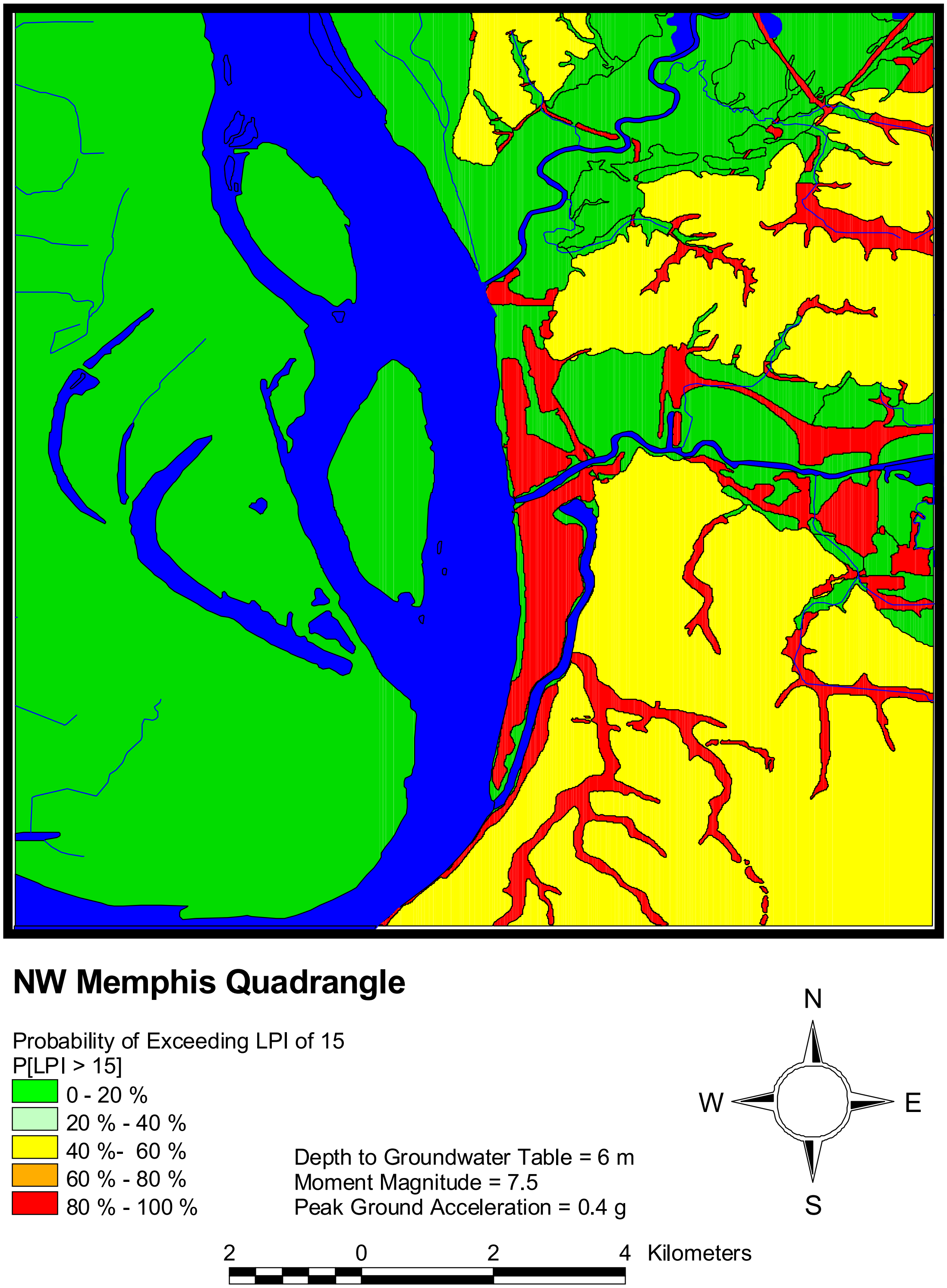

Figure 14 Liquefaction potential map based on liquefaction potential index (LPI) exceeding 15 for NW Memphis quadrangle for a moment magnitude 7.5 and a peak ground acceleration of 0.4 g.

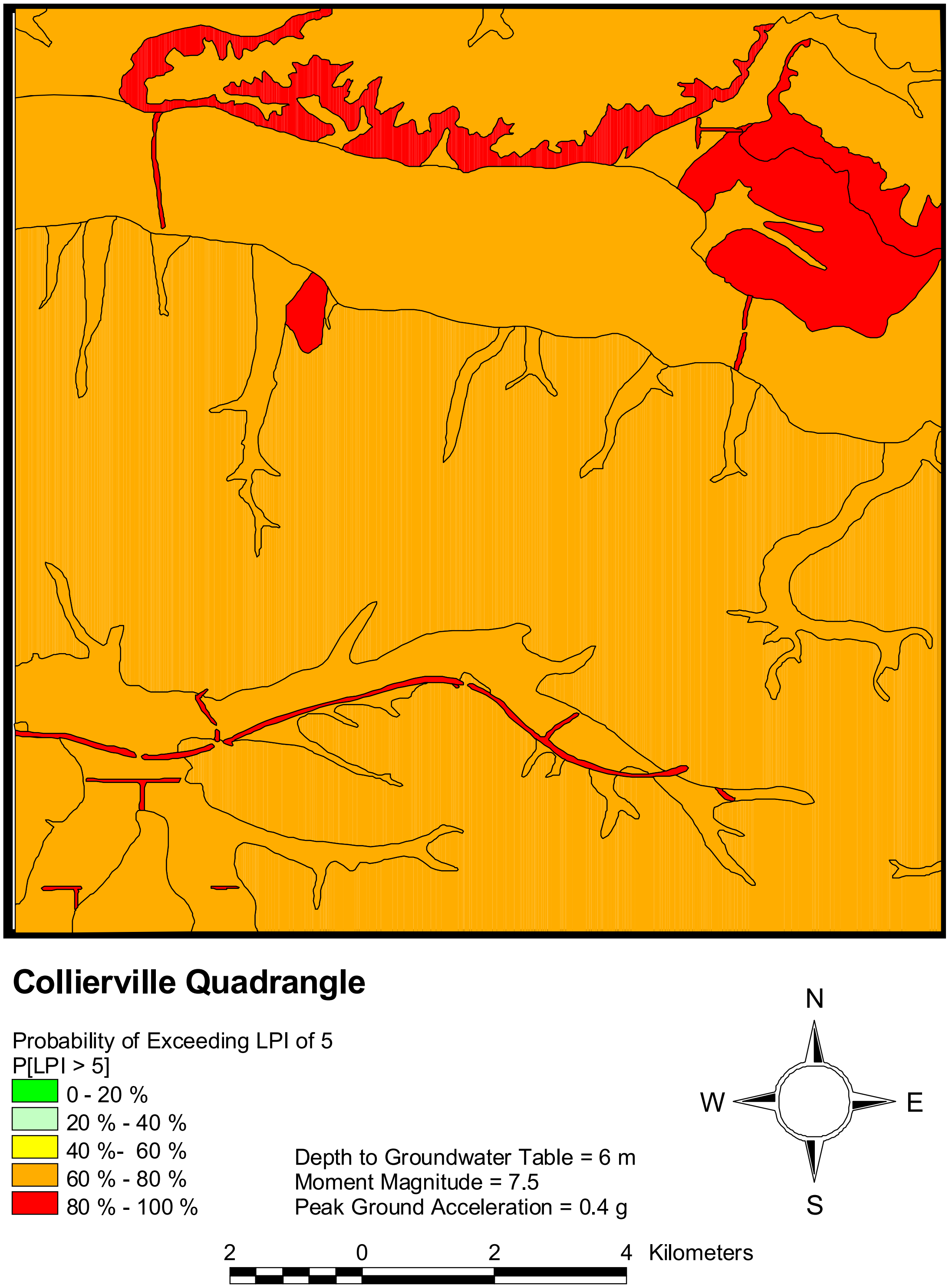

Figure 15 Liquefaction potential map based on a liquefaction potential index (LPI) exceeding 5 for Collierville quadrangle for a moment magnitude of 7.5 and a peak ground acceleration of 0.4 g.

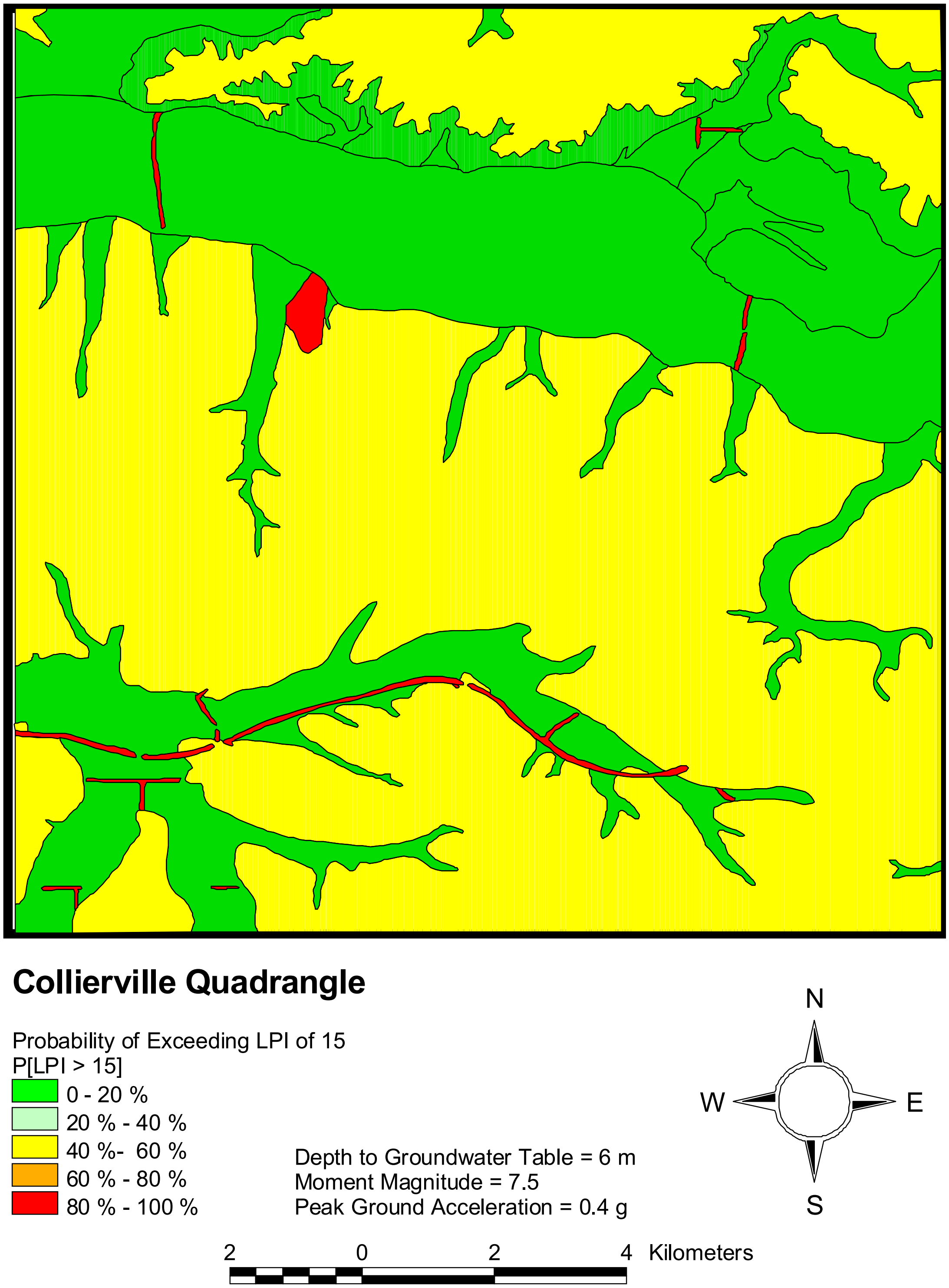

Figure 16 Liquefaction potential map based on a liquefaction potential index (LPI) exceeding 15 for Collierville quadrangle for a moment magnitude of 7.5 and a peak ground acceleration of 0.4 g.

Discussion

The results presented in Table 3 and Figures 13 through 16 indicate that the pleistocene loess deposits have a higher probability of liquefaction-induced damage than do the holocene alluvial deposits, which is the opposite of our expectations. The reason for this is the reliance on a relatively small number of CPT profiles for each geologic unit, particularly for Qtl and Ql. The CPT profiles for the Ql geologic region are based on measurements at only two sites: Shelby Forest and CERI at the University of Memphis. Although the Shelby Forest site is not located within the quadrangles identified by the USGS for the urban seismic hazard maps, it was included in the analysis because of the numerous profiles obtained at this site. The profiles obtained in Shelby Forest are shown in Figure 3 as profiles Ql 5-Ql 8 whereas the CERI profiles are shown as profiles Ql 1- Ql 4. The multimodal distribution observed in Figure 12 for LPI values in Ql regions is due to the distinctly different q_t and f_s profiles measured at the Shelby Forest site and CERI sites. The very narrow distribution for LPI values in Qtl regions in Figure 12 is directly due to the very limited number of CPT profiles available for this unit.

If the Shelby Forest site is assumed to not represent typical Ql regions within the quadrangles of interest and is omitted from the analysis, the probability of exceeding LPI values of 5 and 15 decreases significantly in accordance with our expectations. For example, for a peak ground acceleration of 0.4 g, the probability of exceeding an LPI of 5 decreases from 50% to 0% for a moment magnitude of 6.5 and decreases from 63% to 25% for a moment magnitude of 7.5. Similarly, the probability of exceeding an LPI of 15 for the same peak ground acceleration decreases from 25% to 0% for a moment magnitude of 6.5 and 50% to less than 1% for a moment magnitude of 7.5. The large uncertainty in this analysis is due to the limited CPT available. Revised maps are presented in Figures 17-20 reflecting the omission of the Shelby Forest data.

We propose to address this limitation by (1) calibrating and validating the CPT-based approach using the available CPT soundings from the San Francisco Bay area (Toprack and Holzer, 2003) and (2) using an alternative procedure based on SPT data where the number of profiles is larger (but the data is of a lower quality) and subsequently combining the CPT and SPT results.

References

Deutsch, C.V. and A.G. Journel, (1998). *GSLIB: Geostatistical Software Library and User's Guide*, 2nd Edition, Oxford University Press, New York.

Holzer, T.L., S. Toprak, and M.J. Bennett, (2002). "Application of the Liquefaction Potential Index to Liquefaction Hazard Mapping," *Proceedings*, 8th U.S.-Japan Workshop on Earthquake Resistant Design of Lifeline Facilities and Countermeasures Against Liquefaction, Tokyo, Japan.

Hwang, H., M.-C. Chien, and Y.-W. Lin (1999). Investigation of Soil Conditions in Memphis, Tennessee, USGS Award No. 1434-HQ-98-GR-00002.

Iwasaki, T., F. Tatsuoka, K. Tokida, and S. Yasuda, (1978). "A Practical Method for Assessing Soil Liquefaction Potential Based on Case Studies at Various Sites in Japan," *Proceedings*, 2nd International Conference on Microzonation, San Francisco, 885-896.

Iwasaki, T., K. Tokida, F. Tatsuoka, S. Watanabe, S. Yasuda, and H. Sato, (1982). "Microzonation for Soil Liquefaction Potential Using Simplified Methods," *Proceedings*, 3rd International Conference on Microzonation, San Francisco, 1319-1330.

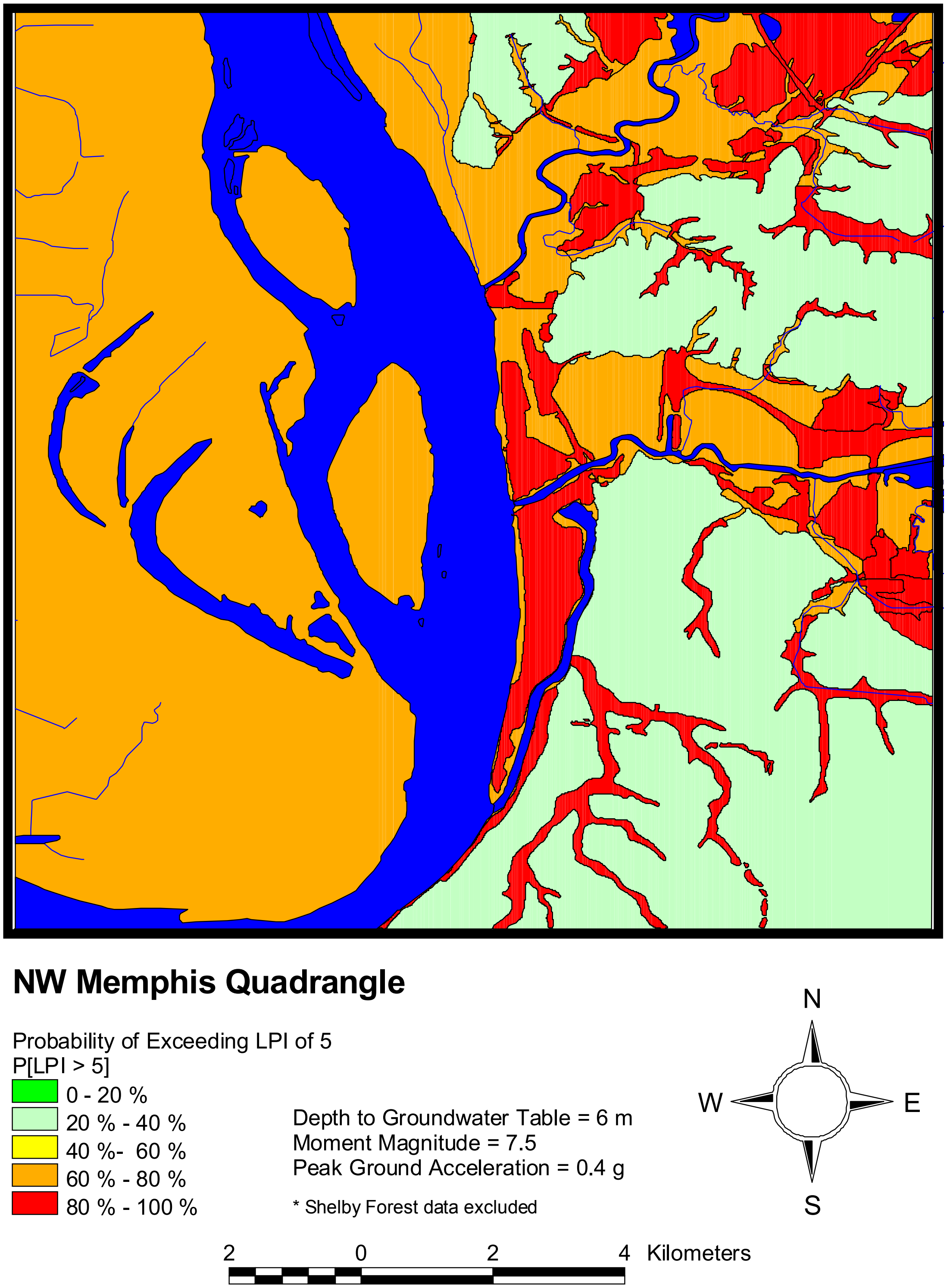

Figure 17 Liquefaction potential map based on liquefaction potential index (LPI) exceeding 5 for NW Memphis quadrangle for a moment magnitude of 7.5 and a peak ground acceleration of 0.4 g. Profiles from Shelby Forest are excluded from the analysis.

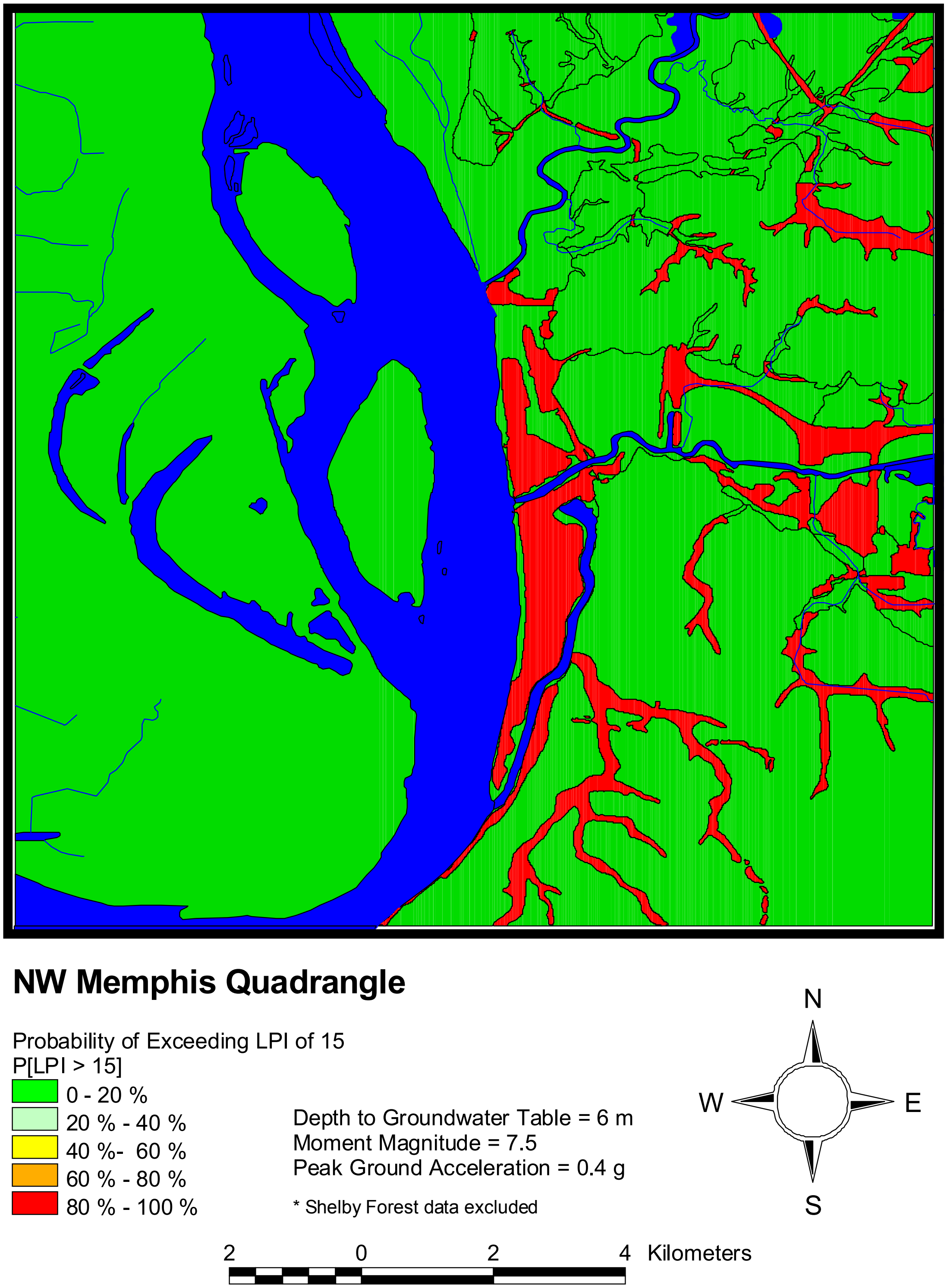

Figure 18 Liquefaction potential map based on liquefaction potential index (LPI) exceeding 15 for NW Memphis quadrangle for a moment magnitude of 7.5 and a peak ground acceleration of 0.4 g. Profiles from Shelby Forest are excluded from the analysis.

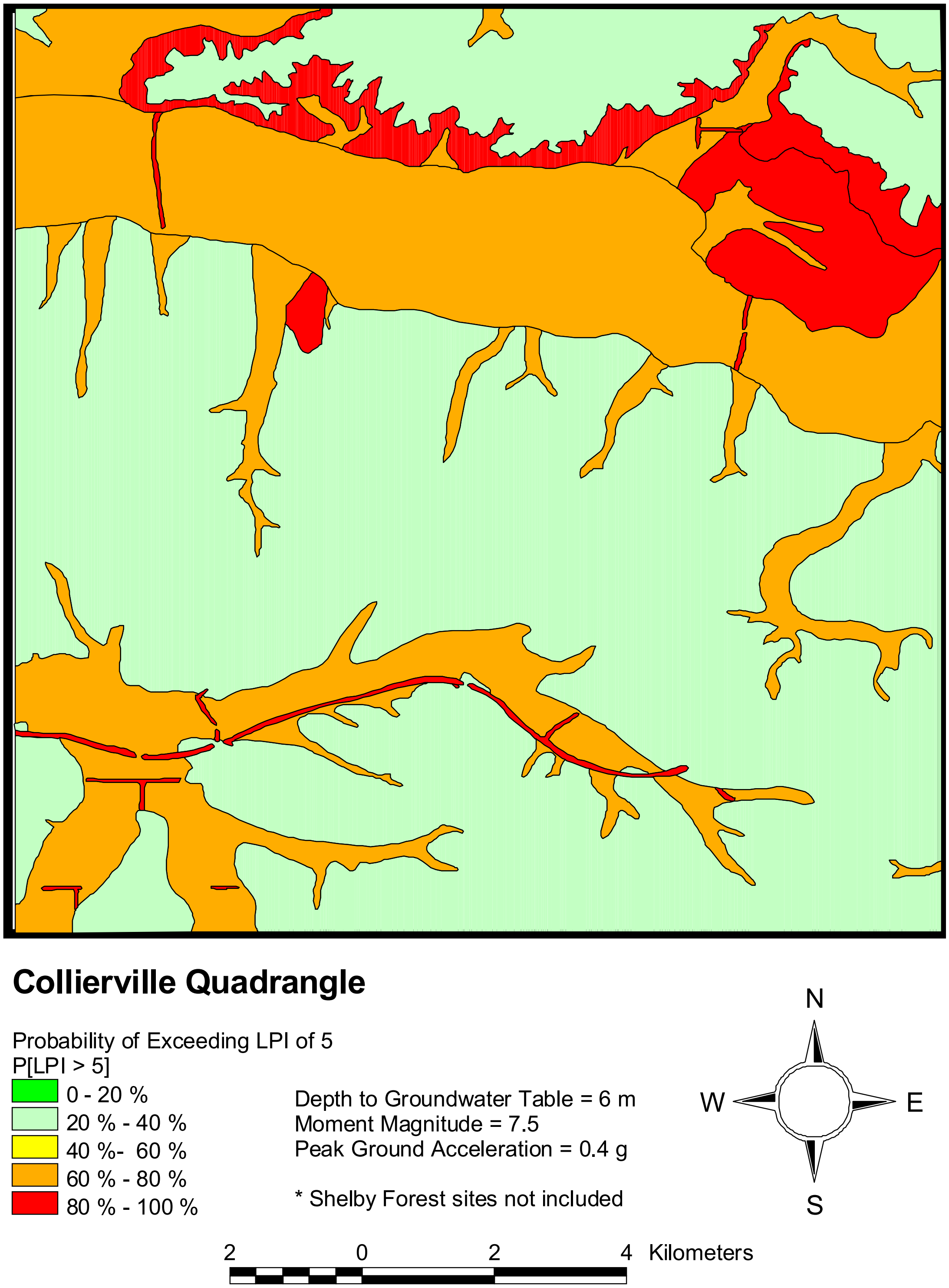

Figure 19 Liquefaction potential map based on liquefaction potential index (LPI) exceeding 5 for Collierville quadrangle for a moment magnitude of 7.5 and a peak ground acceleration of 0.4 g. Profiles from Shelby Forest are excluded from the analysis.

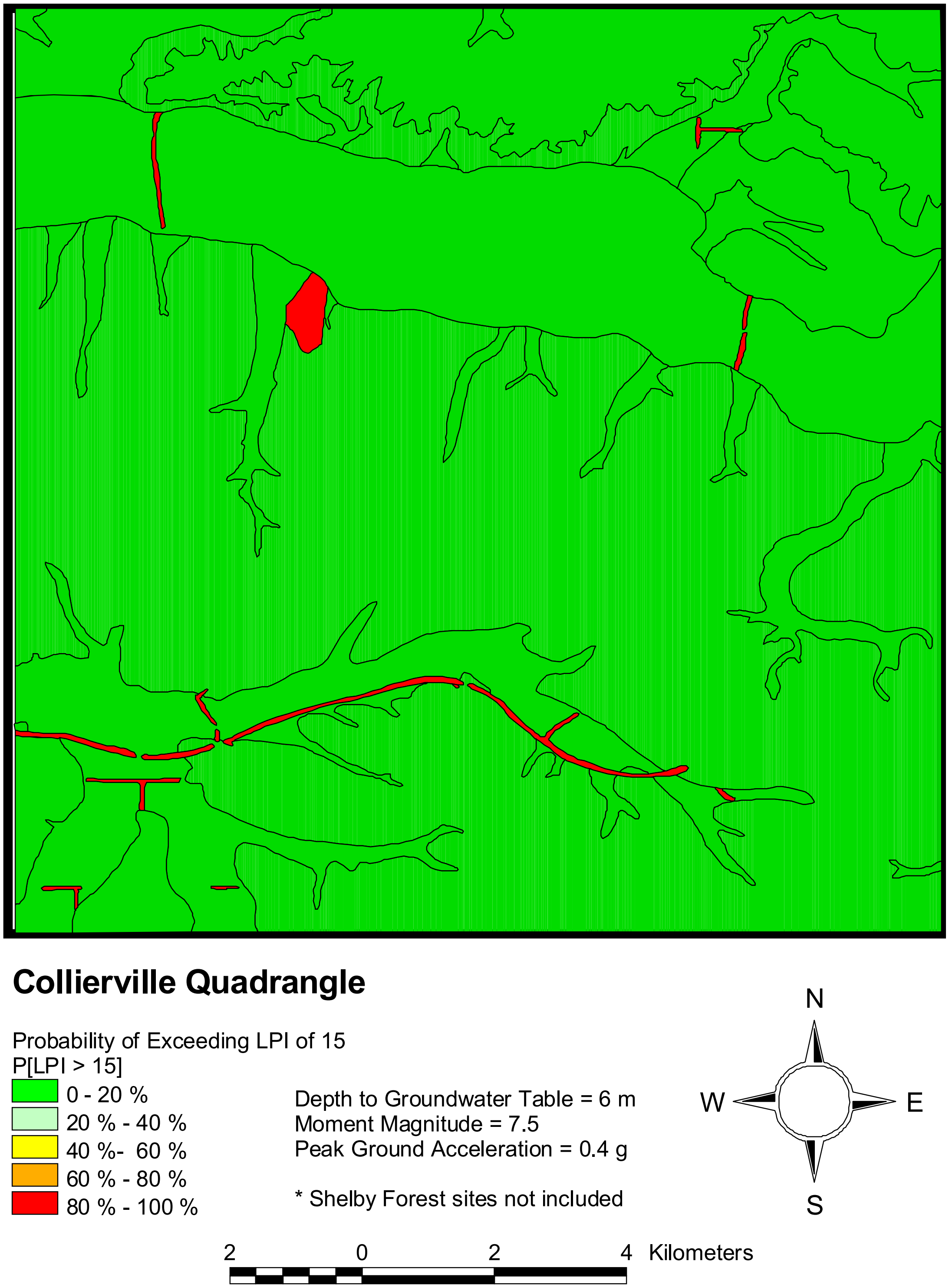

Figure 20 Liquefaction potential map based on liquefaction potential index (LPI) exceeding 15 for Collierville quadrangle for a moment magnitude of 7.5 and a peak ground acceleration of 0.4 g. Profiles from Shelby Forest are excluded from the analysis.

Liao, T., P.W. Mayne, M.P.Tuttle, E.S. Schweig, and R.B. Van Arsdale, (2002). "CPT Site Characterization for Seismic Hazards in the New Madrid Seismic Zone," *Soil Dynamics and Earthquake Engineering*, 22, 943-950

Lin, H., H. Hwang, and T. Chou (1989). *Estimation of Liquefaction Potential and Permanent Ground Deformation Using Neural Network Technology and GIS*, Center for Earthquake Research and Information.

McGillivray, A. (2001). personal communication, Georgia Institute of Technology.

Toprak, S., and T.L. Holzer, (2003), "Liquefaction Potential Index: Field Assessment." *Journal of Geotechnical and Geoenvironmental Engineering*, 129(4), 315-322.

Van Arsdale, R., and R. Cox, (2003). Surficial Geologic and Liquefaction Susceptibility Mapping in Shelby County, Tennessee, Final Technical Report, USGS Award Number 00HQGR0031.

Youd, T.L. I.M Idriss, R.D. Andrus, I. Arango, G. Gastro, J.T. Christian, R. Dobry, W.D.L. Finn, L. F. Harder, Jr., M.E. Hynes, K. Ishihara, J.P. Koester, S.S.C. Liao, W.F. Marcuson, III, G.R. Martin, J.K. Mitchell, Y. Moriwaki, M.S. Power, P.K. Robertson, R.B. Seed, and K.H. Stokoe, II, (2001). "Liquefaction Resistance of Soils: Summary Report from the 1996 NCEER and 1998 MCEER/NSF Workshops on Evaluation of Liquefaction Resistance of Soils." *Journal of Geotechnical and Geoenvironmental Engineering*, 127(10), 817-833.